Magnetic bearing with separate bias and control windings

Ngoc Vu VO* and Hyeong-Joon AHN**
* Department of Mechanical Engineering, Graduate School, Soongsil University
369, Sangdo-ro, Dongjak-gu, Seoui, 06978, South Korea
** School of Mechanical Engineering, Soongsil University
369, Sangdo-ro, Dongjak-gu, Seoui, 06978, South Korea
E-mail: ahj123@ssu.ac.kr

Abstract
Although magnetic bearing (MB) supports the target object without contact, enabling high-efficiency operation, its complex hardware and nonlinear characteristics make control system design challenging. Self-sensing is a signal-processing technique that estimates the position of a levitated object in a MB using current signals. However, conventional self-sensing MB with single winding, where the winding is used for both actuation and sensing, suffers from noise and interference. This paper investigates a self-sensing MB system with separate bias and control windings. The bias winding is used to estimate the air gap of the electromagnet, whereas the control winding is responsible for generating the electromagnetic force. First, a mathematical model of MB with separated windings is derived and compared with that of a conventional MB. The actuator gain and stiffness can be tuned effectively by appropriately adjusting the ratio between the bias and control windings. Furthermore, an electromechanical model and analysis of the proposed MB configuration are presented. In this design, the inductance of the control winding remains nearly constant regardless of the air gap, which facilitates the current control. Additionally, using fewer turns in the bias winding is recommended to improve the resolution of self-sensing and minimize the influence of current control on the bias winding. Finally, one DOF MB test rig was constructed and the concept of a self-sensing MB with separate bias and control winding are experimentally validated.

Keywords : Magnetic bearing, Self-sensing, Separate bias and control winding,

1. Introduction

A magnetic bearing (MB) supports the target object without contact, enabling a high-efficiency operation. It is used in various fields such as turbo machinery, flywheel energy storage systems, and artificial hearts(Schweitzer and Maslen 2009). However, its complex hardware and nonlinear characteristics make control system design challenging. Conventional MBs independently control the currents of two opposing electromagnets around the target object. Although linearization can be achieved using a bias current, the inductance varies with the air gap, and the magnetic force exhibits nonlinear characteristics(Schweitzer and Maslen 2009).

Self-sensing is a signal-processing technique that estimates the position of a levitated object in an MB by using current signals. Many researchers have reported successful approaches using self-sensing techniques(Vischer and Bleuler 1993, Mizuno and Bleuler 1995, Sivadasan 1996, Noh and Maslen 1997, Thibeault and Smith 2002, Schammass and et al. 2005, Park and Jang 2008, Glück and Kugi 2011, Niemann and Du Rand 2013, Wang and Binder 2016, Yoo and et al. 2021). Research has focused on improving the estimation accuracy by addressing challenges such as noise, nonlinearity, and sensitivity to operating conditions through advanced signal processing, winding configurations, and control strategies.

Conventional self-sensing MB with single winding, where the winding is used for both actuation and sensing, suffers from noise and interference. Although a self-sensing MB with separate bias and control windings was proposed based on a differential transformer-type displacement sensor(Matsuda and Tani 1997), the control winding was used for both actuation and sensing. In addition, there was an MB with separate bias and control windings(Le, Wang et al. 2022), which was not for self-sensing.

This study investigated an MB system with separate bias and control windings. The bias winding is used to estimate the air gap of the electromagnet, whereas the control winding is responsible for generating the electromagnetic force. First, a mathematical model of the MB with separated windings is derived and compared with that of a conventional MB. The actuator gain and stiffness can be tuned effectively by appropriately adjusting the ratio between the bias and control windings. Furthermore, an electromechanical model and analysis of the proposed MB configuration are presented. In this design, the inductance of the control winding remains nearly constant regardless of the air gap, which facilitates the current control. Additionally, using fewer turns in the bias winding is recommended to improve the resolution of self-sensing and minimize the influence of current control on the bias winding. Finally, one DOF MB test rig was constructed and the concept of a self-sensing MB with separate bias and control winding are experimentally validated.

2. MB with separate bias and control windings

A conventional MB, as shown in Fig. 1(a), supports the target object without contact by independently controlling the currents of two opposing electromagnetic windings. A conventional MB requires two current drivers to dynamically control the currents. The MB with separate bias and control windings is shown in Fig. 1(b). Each electromagnet has both a bias winding and a control winding. The control windings of the two electromagnets are electrically connected and controlled by a single dynamic current driver. A constant voltage or PWM (v_0) is applied to the two bias windings, ensuring a steady bias current (i_0). Therefore, although two windings are required per electromagnet, the number of current drivers can be reduced by half, as shown in Fig. 1. In a conventional MB, the bias and control windings are electrically connected, whereas in the proposed MB, the bias and control windings are magnetically coupled.

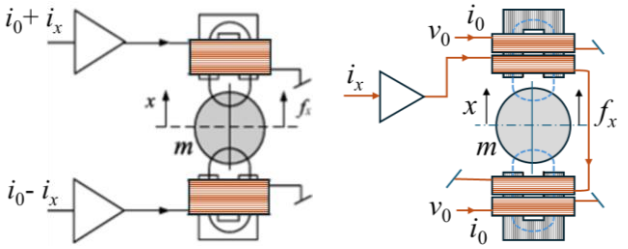

(a) Conventional MB (b) MB with separate windings

Fig. 1 Conventional and proposed MBs

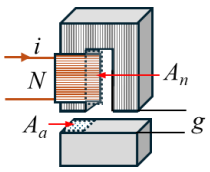

Fig. 2 Electromagnet

$$f = 0.25\mu_0 N^2 i^2 A_a/g^2 = k\, i^2/g^2 \quad (1)$$

Here, $k = 0.25\mu N^2 A_a$

$$L = 0.5\mu_0 N^2 i^2 A_a/g \quad (2)$$

$$R_{cu} = \rho l_m N^2/A_a K_{st} \quad (3)$$

Table 1. Comparison of conventional and proposed MBs

Item	Conventional MB	Proposed MB	
Magneto motive force	Ni	$N_0 i_0 \pm N_c i_c$	$2\alpha N i_0 \pm 2(1-\alpha) N i_c$
Max. current	$i_{max}=2i_0$	$i_{cmax}=i_0$	$i_{cmax}=i_0$
Resistance (R_{cu})	$\rho l_m N^2/A_n K_n \propto N^2$	Bias wndg: $2\rho l_m N_0^2/A_n K_n$ Control wndg: $2\rho l_m N_c^2/A_n K_n$	Bias wndg: $8\alpha^2 N^2 \rho l_m/A_n K_n$ Control wndg: $8(1-\alpha)^2 N^2 \rho l_m/A_n K_n$
Copper loss ($R_{cu}\cdot i_{max}^2$)	$\propto N^2(i_0+i_c)^2 \approx 4N^2 i_0^2$	Bias wndg: $\propto 2N_0^2 i_0^2$ Control wndg: $\propto 2N_c^2 i_c^2 \approx 2N_c^2 i_0^2$ Total: $\propto 2(N_0^2+N_c^2) i_0^2$	Bias wndg: $\propto 8\alpha^2 N^2 i_0^2$ Control wndg: $\propto 8(1-\alpha)^2 N^2 i_c^2 \approx 8(1-\alpha)^2 N^2 i_0^2$ Total: $\propto 8(1-2\alpha+2\alpha^2) N^2 i_0^2$
Nominal inductance	$L=0.5\mu_0 N^2 A_a/g$	Bias wndg: $L_{00}=0.5\mu_0 N_0^2 A_a/g$ Control wndg: $L_{cc}=0.5\mu_0 N_c^2 A_a/g$ Mutual: $L_{c0}=0.5\mu_0 N_c N_0 A_a/g$	Bias wndg: $L_{00}=2\mu_0\alpha^2 N^2 A_a/g$ Control wndg: $L_{cc}=2\mu_0(1-\alpha)^2 N^2 A_a/g$ Mutual: $L_{c0}=2\mu_0\alpha(1-\alpha) N^2 A_a/g$
Electromagnetic force	$f_\pm=0.25\mu_0 N^2(i_0\pm i_c)^2 A_a/(g\mp x)^2$	$f_\pm=0.25\mu_0(N_0 i_0 \pm N_c i_c)^2 A_a/(g\mp x)^2$	$f_\pm=0.25\mu_0(2\alpha N i_0 \pm 2(1-\alpha) N i_c)^2 A_a/(g\mp x)^2$
Current gain	$k_i=\mu_0 N^2 i_0 A_a/g^2$	$k_i=\mu_0 N_0 N_c i_0 A_a/g^2$	$k_i=4\mu_0\alpha(1-\alpha) N^2 i_0 A_a/g^2$
Open-loop stiffness	$k_x=\mu_0 N^2 i_0^2 A_a/g^3$	$k_x=\mu_0 N_0^2 i_0^2 A_a/g^3$	$k_x=4\mu_0\alpha^2 N^2 i_0^2 A_a/g^3$

Neglecting magnetic saturation, Table 1 summarizes the characteristics of conventional and proposed MBs. Here, $f_{\pm}$ represents the forces of the upper and lower electromagnets. As shown in Table 1, if the number of bias and control windings is the same as the total number of windings in a conventional MB (N=N_0=N_c), then the proposed MB exhibits the same characteristics as the conventional MB. Given the same bias and control currents, let the numbers of bias and control windings be $2\alpha N$ and $2(1-\alpha)N$, respectively. The effects of α (variation of winding turns) on the total copper loss, actuator gain (k_i), and stiffness (k_x) are shown in Fig. 3, which are normalized to those of the conventional MB. Because a larger k_i and smaller k_x are advantageous, Fig. 4 presents the relationship between k_i and k_x for different values of α, along with the objective function $k_i/(1.25- k_i)(0.25+ k_x)$, which is roughly proportional to k_i and inversely proportional to k_x. In a conventional MB, α=0.5. The objective function reaches its maximum at α=0.4, where k_i decreases by only 4% to 0.96, whereas k_x decreases considerably by 36% to 0.64.

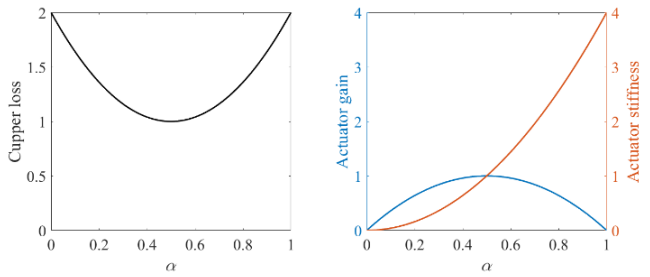

(a) Copper loss (b) Actuator constants

Fig. 3 Cupper loss and actuator constants with various α

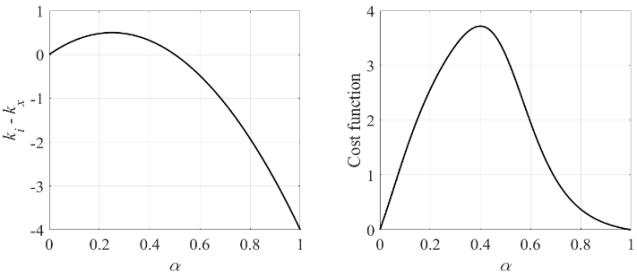

(a) k_i-k_x (b) Cost function

Fig. 4 k_i-k_x and cost function with various α

In Fig. 2, when a current i flows through an electromagnet winding with N turns, the pole area of the electromagnet is A_a, and the air gap between the target object and the electromagnet is g. The electromagnetic force (f) acting on the target object is given by Eq. (1), while the inductance L and resistance R of the winding are given by Eqs. (2) and (3), respectively. Here, μ_0 is the permeability of air, ρ is the resistivity of the winding, A_n is the area between the electromagnet poles for winding, l_m is the average length per turn, and K_{st} is the winding density.

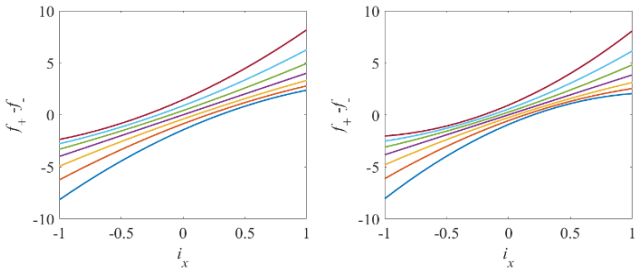

(a) α=0.5 (b) α=0.4

Fig. 5 MB force with various control currents and displacements

3. Dynamic modeling and analysis of MB with separate bias and control windings

The electromagnet with separate bias and control windings can be modeled as a doubly excited linear electromagnet, which is shown in the upper part of Fig. 6. Fig. 6 shows a single degree of freedom (DOF) MB consisting of two electromagnets at both sides of the ferromagnetic object. Using electromechanical energy conversion theory, the amount of electrical energy W_e has been transferred into the magnetic field W_f and converted into the mechanical work W_m. The differential energy and coenergy functions of the upper electromagnet can be derived as Eq. (4). Here, $dW_e = e_{c+}i_{c+}dt + e_{0+}i_{0+}dt$, $e_{c+} = d\lambda_{c+}/dt$, $e_{0+} = d\lambda_{0+}/dt$ and W_m=f_+dx. The reluctance force of the upper electromagnet can be expressed as Eq. (5).

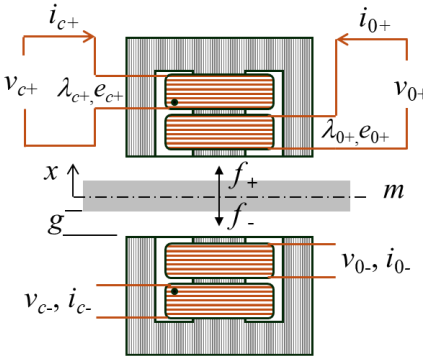

Fig. 6 Dynamic modeling of SDOF MB with separate bias and control windings

$$dW_f = dW_e - dW_m \tag{4}$$

$$f_+ = -\partial W_f(\lambda_{c+}, \lambda_{0+}, x)/\partial x \tag{5}$$

The mathematical model of an electromechanical system comprises circuit equations for the electrical subsystem and

force-balance equations for the mechanical subsystem. The interactions between these two subsystems through the magnetic field are represented by the electromotive forces (emfs) and the electromagnetic force. The electrical equations for the control and bias windings of the upper and lower electromagnets are given by Eqs. (6) and (7), respectively. Here, $L_{cc\pm}=2\mu_0(1-\alpha)^2N^2A_n/(g \mp x)$, $L_{00\pm}=2\mu_0\alpha^2N^2A_n/(g \mp x)$, $L_{c0\pm}=L_{0c\pm}=2\mu_0\alpha(1-\alpha)N^2A_n/(g \mp x)$.

$$\begin{aligned} v_{c\pm} &= R_c i_{c\pm} + d\lambda_{c\pm}/dt = R_c i_{c\pm} + d(\lambda_{cc\pm} \pm \lambda_{c0\pm})/dt \\ &= R_c i_{c\pm} + d(L_{cc\pm} i_{c\pm} \pm L_{c0\pm} i_{0\pm})/dt = R_c i_{c\pm} + L_{cc\pm} di_{c\pm}/dt \pm L_{c0\pm} di_{0\pm}/dt \ (dx/dt \approx 0) \end{aligned} \tag{6}$$

$$\begin{aligned} v_{0\pm} &= R_0 i_{0\pm} + d\lambda_{0\pm}/dt = R_0 i_{0\pm} + d(\lambda_{0c\pm} \pm \lambda_{00\pm})/dt \\ &= R_0 i_{0\pm} + d(\pm L_{0c\pm} i_{c\pm} + L_{00\pm} i_{0\pm})/dt = R_0 i_{0\pm} \pm L_{0c\pm} di_{c\pm}/dt + L_{00\pm} di_{0\pm}/dt \ (dx/dt \approx 0) \end{aligned} \tag{7}$$

The force balance equation for the mechanical system can be expressed as in Eq. (8).

$$m\ddot{x} = f_+ - f_- \tag{8}$$

As the control windings of the upper and lower electromagnets are connected in series, the electric equation can be expressed as Eq. (9), where $v_{c+}=v_{c+}+v_{c-}$ and $i_{c+}=i_{c-}$. his series connection reduces the variation in inductance of the control winding caused by object displacement, as reflected in the term $L_{cc+}+L_{cc-}$. Additionally, if the two bias windings are driven symmetrically, their mutual inductances cancel out near the equilibrium point (x=0), as seen in the term $L_{c0+}di_{0+}/dt - L_{c0-}di_{0-}/dt$. Consequently, the current control of the serially connected control windings becomes significantly easier than that in a conventional MB. Moreover, the current in the bias winding has a minimal influence on the control winding, even when large current ripples are applied to the bias winding to enhance the position estimation accuracy.

$$v_c = 2R_c i_c + (L_{cc+}+L_{cc-})di_c/dt + (L_{c0+}di_{0+}/dt - L_{c0-}di_{0-}/dt) \approx 2R_c i_c + L_c di_c/dt \tag{9}$$

Using Eq. (9), the electric equation of the bias winding can be approximated using Eq. (10). With a fixed duty ratio, the bias current ($i_{0\pm}$) remains constant, allowing the object's displacement to be estimated from the inductance ($L_{00\pm}$) or current slope ($di_{0\pm}/dt$) (Wang and Binder 2016, Yoo and et al. 2021). However, the current in the control winding (i_c) also affects the bias winding current. In other words, the control effort can directly interfere with the position estimation, a phenomenon known as an all-pass system.

$$v_{0\pm} = R_0 i_{0\pm} \pm L_{0c\pm}(v_c - 2R_c i_c)/L_c + L_{00\pm} di_{0\pm}/dt \tag{10}$$

The influence of the control current on the bias current is proportional to both the resistance of the control winding and the ratio between the bias and control windings ($\alpha/(1-\alpha)$). Moreover, a steeper current slope improves the resolution of position estimation when the bias current slope is used. However, reducing the number of turns in the bias winding requires a higher bias current, which necessitates the use of a thicker copper wire.

4. Experiments

We built a one-degree-of-freedom (1-DOF) MB system featuring separate bias and control windings, as shown in Fig. 2. The balance beam is designed to have low moments of inertia and laminated ferromagnetic target. Two coils with separate bias and control windings are shown in Fig. 2(b). Here, α is 1/6. A commercial AEC PU-09 gap sensor was used as a reference. The system was controlled using a DSP TMS320F28379D with two three-phase drivers (BOOSTXL-DRV8323RS) from Texas Instruments. Parameters are summarized in Table 2.

Table 2 Parameters of 1-DOF MB

A_a	μ_r	x	J	l	Magnet	Target	DC link	Carrier
13mm × 17.5mm	7000	-0.25 ~0.25mm	27e3 kgmm^2	156mm	E41	I48	24V	10kHz

Currents in the bias winding, corresponding to variations in the air gap, are measured and shown in Fig. 8(a). The PWM voltage induces a sawtooth-shaped current in the bias winding. The peak-to-peak current varies from 21.3 to 23.7 A, with the corresponding current slopes ranging from approximately 398 to 452 kA/s, as shown in Fig. 8(b). The average current slope is calculated from 16 current samples within a control cycle, and this is used to estimate the air gap. Fig. 8(c) illustrates that the control winding current affects the bias winding current, as described in Eq. (10). However, since the estimated air gap—based on the average current slope of the bias winding—exhibits a linear relationship with the control current, the influence of the control winding current can be easily compensated for in the air gap estimation.

(a) 1-DOF MB system with separate bias and control windings (b) Coils

Fig. 7 Experimental set-up

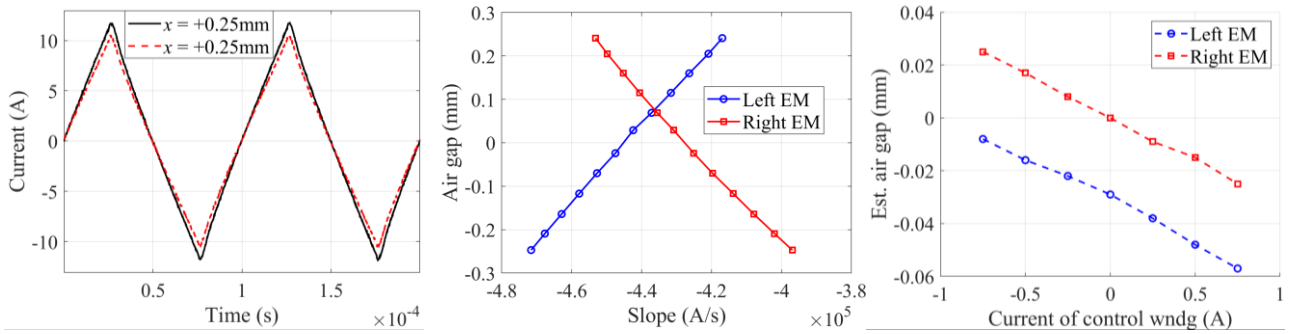

(a) Current of bias winding (b) Average current slope vs air gap (c) Effect of control winding current

Fig. 8 Air gap estimation from average current slope of the bias winding

Static and dynamic performances of the air gap estimation are evaluated by comparing static noise, levitation jitter and closed loop sensitivity function with those obtained using sensor measurement. The static noise of the sensor and self-sensing measurements are compared in Fig. 9(a), standard deviation (STD) of 5.98 and 7.46 μm, respectively. Levitation jitters from both methods are shown in Fig. 9(b), with corresponding STDs of 6.21 and 7.77 μm. These results demonstrate that the self-sensing method with separate bias and control windings achieves performance comparable to that of sensor-based measurements.

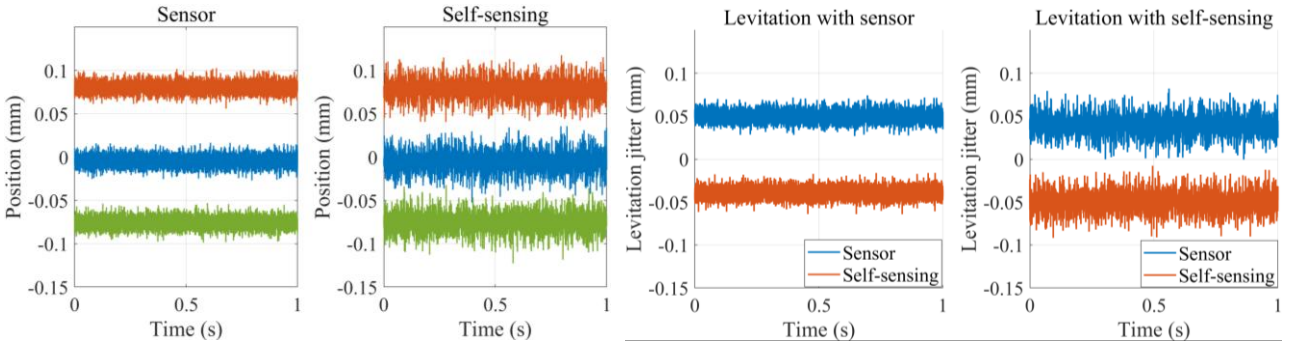

(a) Static noise (b) Levitation jitter

Fig. 9 Static noise and levitation jitter

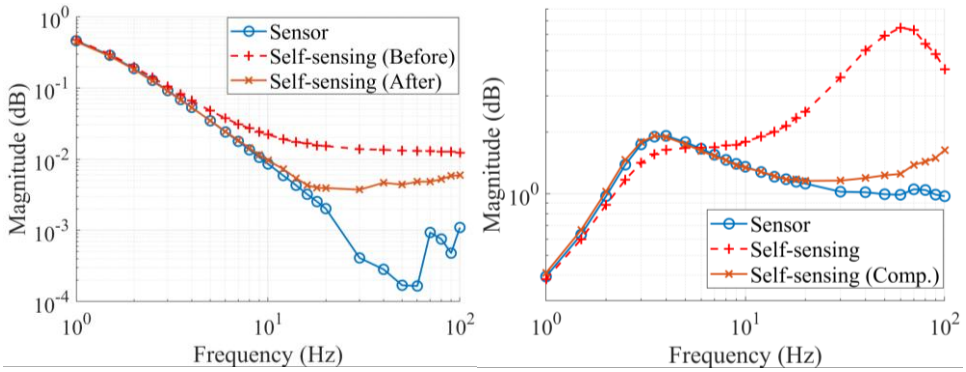

(a) Open-loop plant (b) Closed-loop sensitivity function

Fig. 10 Frequency responses of MB with sensor and self-sensing

Fig. 10(a) compares frequency response of the open-loop plant of MB with sensor and self-sensing. In this context, 'self-sensing (comp.)' indicates that the control winding current has been compensated. The effect of both the control winding current on self-sensing and its compensation can be clearly seen in Fig. 10(a). The closed-loop sensitivity of levitated MB with sensor and self-sensing are shown in Fig. 10(b). After compensation, levitated MBs with sensor and self-sensing exhibit almost identical characteristics below 20 Hz.

5. Conclusion

This study investigated an MB system with separate bias and control windings. The bias winding is used for the air-gap estimation, whereas the control winding is responsible for generating the electromagnetic force. Although each electromagnet requires two windings, the total number of current drivers can be reduced by half. First, a mathematical model of the MB with separate windings is derived and compared with that of a conventional MB. Electromechanical modeling and analysis were conducted to evaluate the characteristics of the system. In this configuration, the inductance of the control winding remains nearly constant, regardless of the air gap, which simplifies the current control. Furthermore, using fewer turns in the bias winding is recommended to enhance the resolution of self-sensing and reduce the influence of the control current on the bias winding. Finally, one DOF MB test rig was constructed and the concept of a self-sensing MB with separate bias and control winding are experimentally validated.

Acknowledgement

This work was supported by the Energy Technology R&D program of the KETEP from the Ministry of Trade, Industry & Energy (RS-2023-00242282).

References

Glück, T. K. W. T. C. and A. Kugi, A novel robust position estimator for self-sensing magnetic levitation systems based on least squares identification, *Control Engineering Practice*, vol. 19, no. 2, pp. 146-157 (2011).

Le, Y., D. Wang and S. Zheng, Design and Optimization of a Radial Magnetic Bearing Considering Unbalanced Magnetic Pull Effects for Magnetically Suspended Compressor, *IEEE/ASME Transactions on Mechatronics*, vol. 27, no. 6, pp. 5760-5770 (2022).

Matsuda, K. O. Y. and J. Tani, Self-sensing magnetic bearing using the differential transformer principle, *Transactions of the Japan Society of Mechanical Engineers Series C*, vol. 63, no. 609, pp. 1441-1447 (1997).

Mizuno, T. and H. Bleuler, Self-sensing magnetic bearing control system design using the geometric approach, *Control Engineering Practice*, vol. 3, pp. 8 (1995).

Niemann, A. C. V. S. G. and C. P. Du Rand, A self-sensing active magnetic bearing based on a direct current measurement approach, *Sensors*, vol. 13, no. 9, pp. 12149-12165 (2013).

Noh, M. D. and E. H. Maslen, Self-sensing magnetic bearings using parameter estimation, *IEEE Transactions on Instrumentation and Measurement*, vol. 46, pp. 45-50 (1997).

Park, Y. H. H. D. C. P. I. H. A. H. J. and D. Y. Jang, A self-sensing technology of active magnetic bearings using a phase modulation algorithm based on a high frequency voltage injection method, *Journal of Mechanical Science and Technology*, vol. 22, no. 9, pp. 1757-1764 (2008).
Schammass, A. H. R. B. P. and et al., New results for self-sensing active magnetic bearings using modulation approach, *IEEE Transactions on Control Systems Technology*, vol. 13, pp. 509-516 (2005).
Schweitzer, G. and E. Maslen (2009). Magnetic Bearings: Theory, Design, and Application to Rotating Machinery, Springer.
Sivadasan, K. K., Analysis of self-sensing active magnetic bearings working on inductance measurement principle, *IEEE Transactions on Magnetics*, vol. 32, pp. 329-334 (1996).
Thibeault, N. and R. Smith, Magnetic bearing measurement configurations and associated robustness and performance limitations, *Journal of Dynamic Systems, Measurement and Control*, vol. 124, pp. 589-598 (2002).
Vischer, D. and H. Bleuler, Self-sensing active magnetic levitation, *IEEE Transactions on Magnetics*, vol. 29, no. 2, pp. 1276-1281 (1993).
Wang, J. and A. Binder (2016). The Current Slope Based Position Estimation for Self-Sensing Magnetic Bearings, Shaker Verlag GmbH.
Yoo, S. J. K. S. C. K. H. and et al., Data-driven self-sensing technique for active magnetic bearing, *International Journal of Precision Engineering and Manufacturing*, vol. 22, pp. 1031-1038 (2021).